Analytica Chimica Acta 1010 (2018) 1–10

Contents lists available at ScienceDirect

Analytica Chimica Acta

journal homepage: www.elsevier.com/locate/aca

Preparation of molecularly imprinted polymer nanobeads for selective sensing of carboxylic acid vapors

Chuanjun Liu [a, b, *], Liang Shang [a], Hiro-Taka Yoshioka [a], Bin Chen [c], Kenshi Hayashi [a]

[a] Graduate School of Information Science and Electrical Engineering, Kyushu University, 744, Motooka, Nishi-ku, Fukuoka 819-0395, Japan
[b] Research Laboratory, U.S.E. Co., Ltd., 22-10 Ebisu 4-Chome Shibuya-ku, Tokyo 150-0013, Japan
[c] Key Laboratory of Luminescent and Real-time Analytical Chemistry, Ministry of Education, College of Electronic and Information Engineering, Southwest University, Chongqing 400715, China

HIGHLIGHTS

- Molecularly imprinted nanobeads prepared for sensing of typical carboxylic acid vapors in human body odor.
- Nanosize and imprinting effect makes the MIP-beads highly sensitive to vapors at the ppm level.
- MIP-nanobead-coated QCM sensor array developed for the vapor recognition.
- A 96% classification rate achieved by applying Leave-One-Out Cross-Validation on the model of linear discrimination analysis.
- MIP-nanobeads show promise as artificial receptors for vapor and odor sensing.

GRAPHICAL ABSTRACT

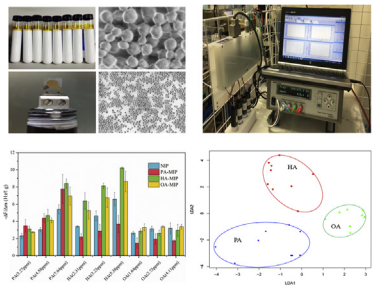

ARTICLE INFO

Article history:
Received 23 November 2017
Accepted 8 January 2018
Available online 30 January 2018

Keywords:
Molecularly imprinted polymer
Quartz crystal microbalance
Nanobeads
Sensor array
Carboxylic acid vapor
Human body odor

ABSTRACT

The detection and discrimination of volatile carboxylic acid components, which are the main contributors to human body odor, have a wide range of potential applications. Here, a quartz crystal microbalance (QCM) sensor array based on molecularly imprinted polymer (MIP) nanobeads is developed for highly sensitive and selective sensing of typical carboxylic acid vapors, namely: propionic acid (PA), hexanoic acid (HA) and octanoic acid (OA). The MIP nanobeads were prepared by precipitation polymerization with methacrylic acid (MAA) as a functional monomer, trimethylolproane trimethacrylate (TRIM) as a crosslinker, and carboxylic acids (PA, HA and OA) as the template molecules. The precipitation polymerization resulted in nano-sized (150–200 nm) polymer beads with a regular shape. The polymerization conditions were optimized to give a functional monomer, crosslinker, and template ratio of 1:1:2. We investigated the imprinting effect using both QCM and GC/MS measurements comparing vapor absorption characteristics between the imprinted and non-imprinted (NIP) nanobeads. A four-channel QCM sensory array based on the NIP and the three types of MIP nanobeads was fabricated for sensing the three types of carboxylic acid vapor at concentrations on the ppm level. The output of the sensor array was analyzed by both a non-supervised method (principle component analysis: PCA) and supervised method (linear discrimination analysis: LDA). LDA showed a better discrimination ability than PCA. A 96%-classification rate was achieved by applying leave-one-out cross-validation to the LDA model. The

* Corresponding author. Graduate School of Information Science and Electrical Engineering, Kyushu University, 744, Motooka, Nishi-ku, Fukuoka 819-0395, Japan.
E-mail address: liu@o.ed.kyushu-u.ac.jp (C. Liu).

https://doi.org/10.1016/j.aca.2018.01.004

high sensitivity and selectivity of the sensor array was attributed to the imprinting effect of the nano-sized polymer beads. The developed MIP nanobeads, together with other types of MIPs, show promise as materials for artificial receptors in vapor and odorant sensing.

1. Introduction

The nature of volatile carboxylic compounds emitted from the human body is determined by many complicated factors such as health status, hereditary features, food habits, gender, and age [1–11]. Human body odor has been shown to contain formation related to the body chemistry of individuals. Thus, assaying human body odor has attracted much research interest in many fields such as cosmetics, biometric, medical diagnosis, forensics, and rescue services. Many chemical compounds, including carboxylic acids, aldehydes, alcohols, ketones, esters, and hydrocarbons, have been identified as major contributors to body odor [12–16]. Among these, carboxylic acids are considered to be key components of body odor. For example, low molecular weight acids, such as acetic acid, propionic acid, isobutyric acid, butyric acid, isovaleric acid, and 3-methyl-2-hexanoic acid, are generally the most-abundant odorants in sweat odor. These molecules have a very low odor threshold and are responsible for the odors of armpits, the scalp, and foot sweat [17–19]. Sweat with a characteristic “acid” odor is categorized by some researchers as one of the three representative types of armpit odor (the other two being “milky” and “cumin”) [20,21]. As the main byproducts of metabolic processes of certain bacteria, volatile carboxylic acids are considered to be vapor biomarkers related to specific diseases [22–27]. Furthermore, different types of bacteria have been reported to produce characteristic mixtures of volatile carboxylic acids. Therefore, it is possible to make a differentiation between bacterial species by analysis of the volatile carboxylic acid composition, and to use them as important discriminators in the generation of body-odor differences [28].

Although the analysis of volatile carboxylic acids may have potential applications in many fields, their detection and discrimination has received little attention. GC/MS is a commonly used analysis method for the measurement of human body odor [29]. However, owing to its high cost and complicated operation skills, its application is limited to the laboratory level. As an alternative, considerable efforts have been made in recent years to develop sensors that can be used for the detection of human body odor. Although there has been little research related to sensing of volatile carboxylic acids, Ko et al., have reported that amine functionalized polypyrrole nanotubes are effective transducers for volatile acetic acid [30]. Lewis et al. reported the detection and classification of carboxylic acids based on carbon black-insulator polymer composites [31–33]. Focusing on visual sensing of human body odor, we have recently developed a pH-sensitive fluorescent imaging sensor, which successfully visualized volatile carboxylic acid in body sweat [34,35]. The carboxylic acid molecules contained in body odor feature various structures (short and long chain, straight and branched), low concentrations (ppm or ppb levels), and from a complex mixture with interference components. However, the sensitivity and selectivity of reported sensors have yet to meet the performance requirements for sensing real human body odor samples.

Considerable attention has been paid to odor sensing based on gravimetric techniques, such as quartz crystal microbalance (QCM), surface acoustic wave (SAW) and film bulk acoustic resonators (FBARs). In these sensing devices a piezoelectric effect is used to achieve high intrinsic sensitivity. Moreover, a wide variety of sensing materials can be coated on the device to fabricate multi-channel sensing arrays, which greatly enhance the pattern recognition ability of specific odorant molecules from a complex mixture. These features make these systems highly suitable for the detection and discrimination of vapor/odorant molecules [36–40]. Hence, we recently have attempted to detect carboxylic acid vapor using a QCM sensor array coated with molecularly imprinted polymer (MIP) films [41]. Unlike conventional coating materials, a MIP array technique was firstly used to prepare the sensing film on the QCM electrode. The MIP sensing layers were prepared by coating a polymer solution containing polyacrylic acid (PAA) as a host and carboxylic acid molecules as the template. The imprinting ability derived from hydrogen bonding interactions between the PAA host and the acid template molecules. Combined with data analysis techniques, such as principal component analysis (PCA) and support vector machine (SVM), the MIP-based QCM sensor array showed a high recognition for volatile carboxylic acids with both single and mixed components. Although the MIP technique was shown to be effective for carboxylic acid vapor recognition, the concentration of the investigated samples in the previous work was at a level of several tens to hundreds ppm, which is far from the real concentration of carboxylic acids in human body odor. Therefore, it is necessary to further enhance the sensitivity of MIP materials to enable their application to recognition of volatile carboxylic acid components.

The present study investigates the response characteristics of a QCM sensor array coated with MIP nanobeads. The MIP nanobeads were prepared by precipitation polymerization in the presence of template molecules. Precipitation polymerization is a heterogeneous polymer process in which monomers and initiators are dissolved in a solvent but the formed polymer is insoluble and thus precipitates [42–44]. Compared with MIP monolith materials prepared with bulk polymerization, the MIPs prepared by precipitation polymerization give micro- and nano-particles with an imprinting effect, which thus avoids the time-consuming process of grinding and sieving. In addition, the obtained monodisperse particles are regularly shaped and have a high surface area-to-volume ratio, which is convenient for their application to target binding in column analysis or other applications. Therefore, there has been great interest in the preparation and application of micro-/nano-sized MIP materials [45,46]. The detection targets of MIP materials are generally large biological molecules and other chemicals; however, less attention has been paid to recognition of small molecules such as odorants and vapors [47,48]. One purpose of this study is to validate the effectiveness of MIP nanobead materials in the sensing of volatile components (carboxylic acids) contained in human body odor.

Three carboxylic acid molecules, including propionic acid (PA), hexanoic acid (HA) and octanoic acid (OA) were targeted in this study because these are typical components found in human body odor [6,12,13]. The preparation conditions, i.e., molar ratio between functional monomer, crosslinker and template were investigated to optimize the imprinting ability of the nanobeads. The MIP effect of the nanobeads was confirmed by SPME-GC/MS measurements. The polymer nanobeads imprinted with different templates were drop-

coated on QCM electrodes to fabricate a sensor array. Compared with previously reported sensors based on MIP films, the MIP nanobead sensor showed improved sensitivity and selectivity for carboxylic acid vapors with concentrations as low as the ppm level. We attribute this performance to the high specific surface area of the nano-sized MIP beads. The response of the sensor array was analyzed by principle component analysis (PCA) and linear discrimination analysis (LDA). A 96% classification rate was achieved through the use of the leave-one-out cross-validation technique for the LDA model, indicating the good potential for the MIP nanobead-based QCM sensor array in applications related to detection and characterization of human body odor.

2. Experimental

2.1. Materials

Methacrylic acid (MAA), trimethylolprane trimethacrylate (TRIM), azodiisobutyronitrile (AIBN), acetonitrile, and hydrochoric acid (HCl) were analytical reagent and purchased from Wako Pure Chemical Industries, Ltd. (Japan). All chemicals were used as received.

2.2. Preparation of MIP nanobeads

The MIP nanobeads were prepared according to a precipitation polymerization process reported by Ye and Mosbach [42,43]. The polymerization was performed using MAA as the functional monomer, TRIM as the crosslinker, AIBN as the initiator, and carboxylic acid molecules (PA, HA and OA, separately) as the template. In a typical procedure, 30 mL of anhydrous acetonitrile containing 156 μL MAA (1.85 mmol), 591 μL TRIM (1.85 mmol), 10 mg AIBN (0.06 mmol) and a certain amount of the template molecules were place in a borosilicate glass tube equipped with a screw cap. The solution in the tube was purged with nitrogen for 5 min, and then sealed under nitrogen atmosphere. The polymerization was initiated by placing the tube in a water bath at 60 °C for 12 h. The precipitated beads were collected by centrifugation of the suspension solution at 10000 rpm for 10 min. The polymer beads were then immersed for 1 h in 30 mL methanol solution containing 10% acetic acids (v/v%), followed by repeated centrifugation and washing with 30 mL methanol 3 times and finally with acetone 1 time. The beads were dried under vacuum at 50 °C for at least 12 h. Investigation by SPME-GC/MS measurements confirmed that this process effectively removed the template molecules from the beads. The non-imprinted (NIP) beads were prepared and treated by the same process, except that no template molecule was used in the polymerization. A scanning electron microscope (SEM, SU8000, Hitachi, Japan) was used to analyze the morphological characteristics of the nanobeads.

2.3. SPME-GC/MS measurements

The absorption characteristics of the MIP nanobeads were evaluated by SPME-GC/MS with the use of the procedure illustrated in Fig. 1. Carboxylic acid vapors were introduced into a stainless-steel chamber with a volume of 0.3 L. A 1-g portion of the nanobead powder samples set in an aluminum crucible was placed in the chamber for the vapor absorption. After 1 h of absorption, the samples were transferred to a vial for measurement of GC/MS (QP2010SE, Shimadzu, Japan). Divinylbenzene/carboxen on polydimethylsiloxane (CAR/DVB on PDMS) 50/30 μm fiber (SUPELCO, Bellefonte, PA, USA) was used as the SPME probe for auto-sampling. The column used in the GC/MS was a 60 m × 0.32 mm, 0.5-μm film thickness DB-WAX and the carrier gas was helium. The extraction

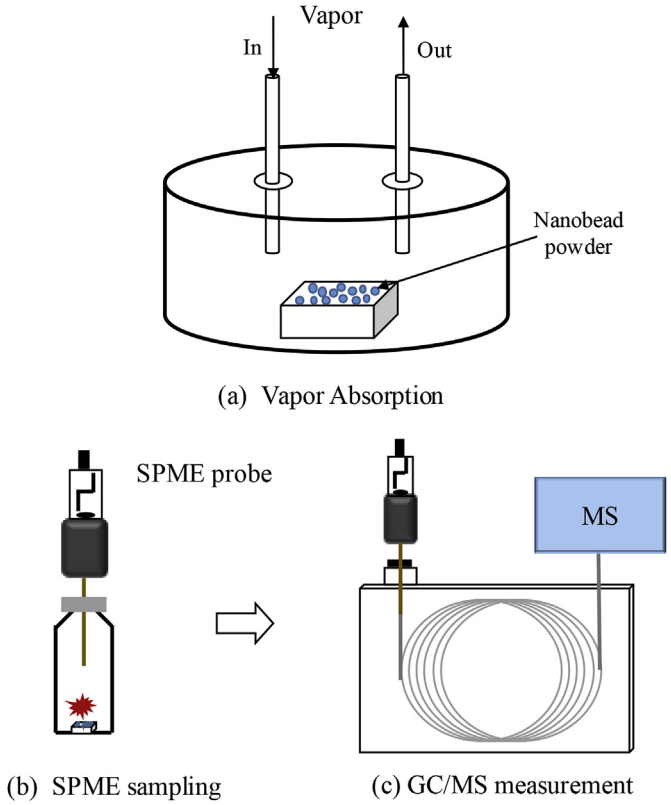

Fig. 1. Schematic diagram of setup in the SPME-GC/MS measurement.

conditions of the SPME probe were 90 °C and 15 min. The SPME probe was desorbed in the injection port at an inlet temperature of 230 °C. A 30-min program began with an initial oven temperature of 40 °C for 5 min, followed by a ramp of 10 °C/min to 230 °C, and ended with a 6-min hold. The quadruple mass analyzer was operated in electron ionization mode, and the scan range was 35–550 *m*/*z*.

2.4. Vapor sensing of QCM sensor array

We used 9 MHz AT-cut quartz crystal electrodes embedded between vacuum-deposited Au (0.5 cm diameter) in this study. The nanobead samples (one NIP and three MIPs with PA, HA, and OA as templates) were dispersed in ethanol, and a total of 5 μL of the suspensions were drop-coated on both sides of the electrode (2.5 μL × 2). The coated electrodes were then dried under vacuum at room temperature before the vapor sensing experiment. A vapor generation system was fabricated to supply vapors at standard concentrations. As shown in Fig. 2a, the system consisted of an air pump (LV-125A, Lincoln, Japan), an air-filtering tube filled with molecular sieves and activated carbon, two mass flow controllers (MFC) (3660, Kofloc, Japan), a three-way solenoid valve (3WSV) (FSM-0408Y, FLON Industry, Japan) and a standard gas generator (PD-1B-2, GASTEC Corporation, Japan). The flow system was controlled through a data acquisition (DAQ) (USB-6009, National instruments, Austin, USA) and LabView software (National instruments, Austin, USA). Vapors with different concentrations were generated by selecting different flow rates (0.3, 0.4 and 0.5 L/min), chamber temperatures (30 or 50 °C) and diffusion tubes (D-20 or D-30). The concentration of the vapors was calculated according to the following equation:

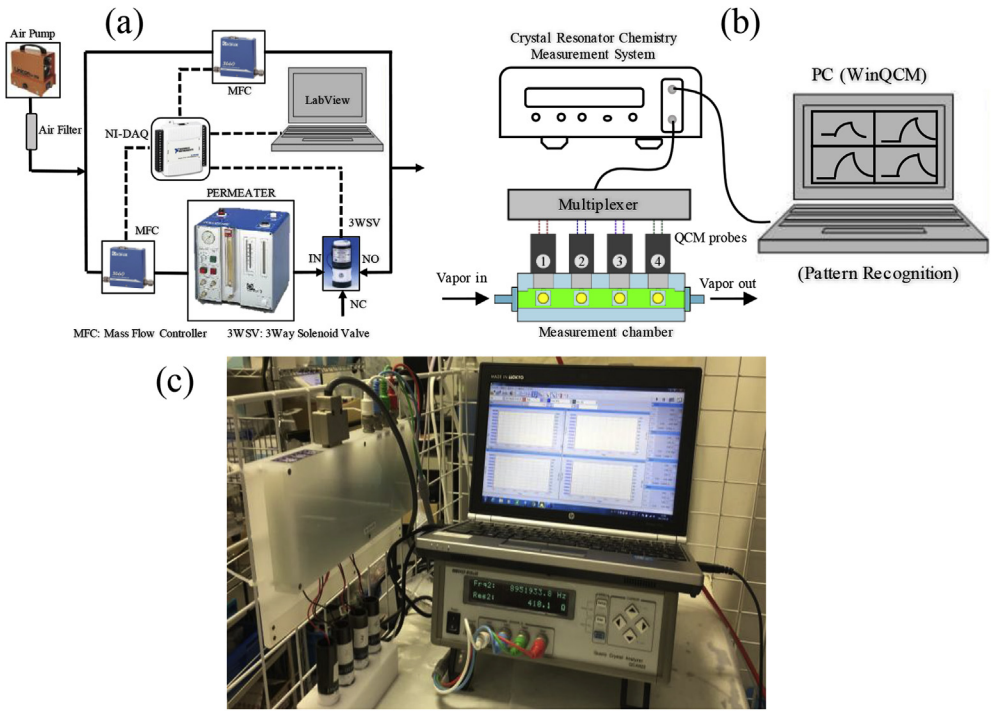

Fig. 2. Schematic diagram of the vapor generation system (a) and the multiple QCM measurement system (b). (c) shows the prototype of the QCM sensing equipment.

$$C = \frac{K \times D_r \times 10^3}{F},$$

where C (ppm) is the concentration of the generated vapor, D_r (μg/min) is the diffusion rate at the set temperature, F (mL/min) is the flow rate of the diluent gas, and K is the factor for converting gas weight to gas volume, which could be calculated as:

$$K = \frac{22.4}{M} \times \frac{273 + t}{273} \times \frac{760}{P},$$

where M is molecular weight, T is the thermodynamic temperature, and P is 760 mmHg. The diffusion rates were measured to be 2.58 μg/min for PA (D-20/30 °C), 7.10 μg/min for HA (D-30/50 °C) and 3.54 μg/min for OA (D-30/50 °C). Compared with the vapor generation method reported in our previous work [41], this system can supply concentrations at the ppm level more accurately (as shown later). A Teflon sensing chamber was used to fix the four QCM probes. The frequency change of the sensor array was measured with a crystal resonator chemistry measurement system and specialist software WinQCM (QCA 922, Seiko EG&G, Japan). A schematic diagram and photograph of the multiple QCM analyzer system are shown in Fig. 2b and c, respectively. The "stats" package of open source language 'R' was used for the PCA and LDA analysis of the response output of the sensor array.

3. Results and discussion

3.1. Morphology and characteristics of MIP-nanobeads

Fig. 3a shows the morphology of the HA-templated beads observed with a scanning electron microscope (SEM). The image was acquired at 120,000 × magnification in secondary electron imaging mode. Polymer beads presented with a regular shape with an average size ranging from 150 to 200 nm. The use of different templates (PA, HA, and OA) had no influence on the fine structure of the MIP nanobeads. Additionally, no obvious differences were observed in the morphology and size distribution between the MIP and NIP nanobeads. The photo of the QCM electrode demonstrated that drop-coating resulted in a nanobead layer with good adhesion to the electrode surface (Fig. 3b). This result was also confirmed by the low resistance of the coated electrode (several tens of ohms). This good film-forming property is a notable advantage of the prepared nanobeads. We have previously tried to use QCM to evaluate the absorption characteristics of monolithic MIP particles prepared by bulk polymerization [34]; however, these experiments failed owing to their poor film-forming character. For the ground monolithic MIP materials, additional adhesive agents are generally needed to immobilize the particles and to prevent the motional losses of the QCM electrode. The use of adhesive should be avoided because these might affect the absorbance characteristics of the sensitive layer. We suggest that the good adhesion might derive from the size effects and the surface character of the nanobeads. The regular shape and nanosize promote the spreading of the beads on the electrode surface. Furthermore, the gel character of the solution precipitated beads might increase interactions between the beads and the electrode surface as well as neighboring beads [42,43].

3.2. Relationship between sensitivity and coating amount

The mass and the thickness of the sensing film influence the intensity and sensitivity of QCM sensors. Before evaluation of the absorption characteristics, we first investigated the response of the electrodes coated with nanobead suspensions at different concentrations. Taking the HA-MIP nanobead as an example, we investigated its response to the HA vapor. As shown in Fig. 4, the increase in the concentration of nanobeads resulted in an increase in the frequency shift ($-\Delta F$) and a decrease in the sensitivity. There existed a variation in fundamental resonant frequency of individual QCM devices. Moreover, it was difficult to guarantee a same coating

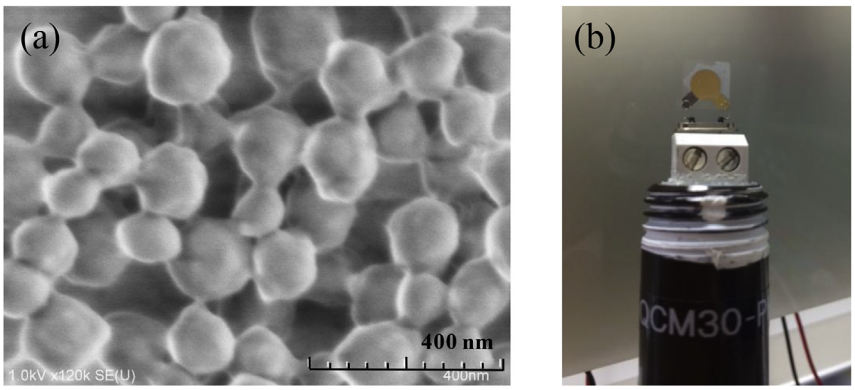

Fig. 3. SEM images of HA-MIP nanobeads (a) and photo of a nanobead-coated QCM electrode (b).

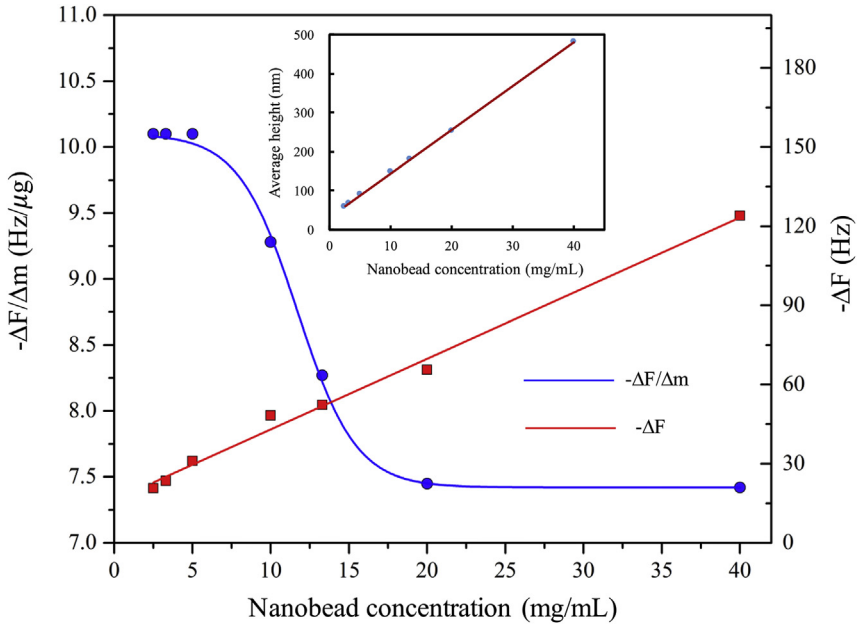

Fig. 4. Coating amount dependent frequency shift (-ΔF) and sensitivity (-ΔF/Δm) of the HA-MIP nanobead-coated QCM electrode upon exposure to the HA vapor (3.23 ppm). Insert shows the average height of the nanobead layer tentatively calculated according to the coating amount.

amount for all electrodes although the concentration of nanobead suspension is the same. Therefore, there always existed a variation in the inherent sensitivity for each coated QCM electrode. In order to reduce this variation as much as possible, the sensitivity of the sensor was normalized here by the frequency shift per unit mass (-ΔF/Δm). The mass (Δm) was calculated by the frequency difference between the coated electrode and the bare counterpart. According to the device characteristics of the used QCM electrode (9 MHz), a 1-Hz change of ΔF corresponds to ca. 1.07 ng of Δm. The frequency shift (−ΔF) was calculated from the frequency difference of the coated electrode between the start and the end of vapor exposure (the time of vapor exposure was 10 min). The concentration dependent decrease in sensitivity derived from the stacking state of the nanobeads on the electrode surface. This assumption was confirmed from SEM images of electrodes coated by nanobead suspensions with different concentrations (Fig. 5). As the coating concentration was increased, the coverage of the nanobeads changed from a scattered distribution to a dense accumulation. An excessive coverage (thick multilayer film) would hinder the effective absorption of the vapors to the nanobeads and cause the frequency response to deviate from the Sauerbrey equation, thus decreasing the sensitivity of the sensors. The insert in Fig. 4 presents the average height of the nanobead layer on the electrode surface. The average height was tentatively calculated according to the amount of coated nanobeads (Δm of two sides), the surface area of the electrode (5 mm in diameter) and a model of hexagonal close-packing with a space fraction of 0.74. The average height of the layer increased linearly from 60 to 480 nm when the nanobead concentration increased from 2.5 to 40 mg/mL. The average height of the layer coated with a concentration of 10 mg/mL was ca. 150 nm, which was roughly equivalent to the diameter of the nanobeads. This result might indicate a monolayer stacking of the nanobeads and was basically consistent with the coating amount of nanobeads as observed in Fig. 5b. Although a low concentration coating corresponds to a high specific sensitivity, the absolute frequency change of the film was low, which might introduce noise into the sensor array and thus influence the discrimination ability. This is a common problem in pattern recognition of electronic nose. Considering the balance between the sensitivity and selectivity, a concentration of 10 mg/mL was applied in the subsequent experiments to prepare the QCM sensor electrode.

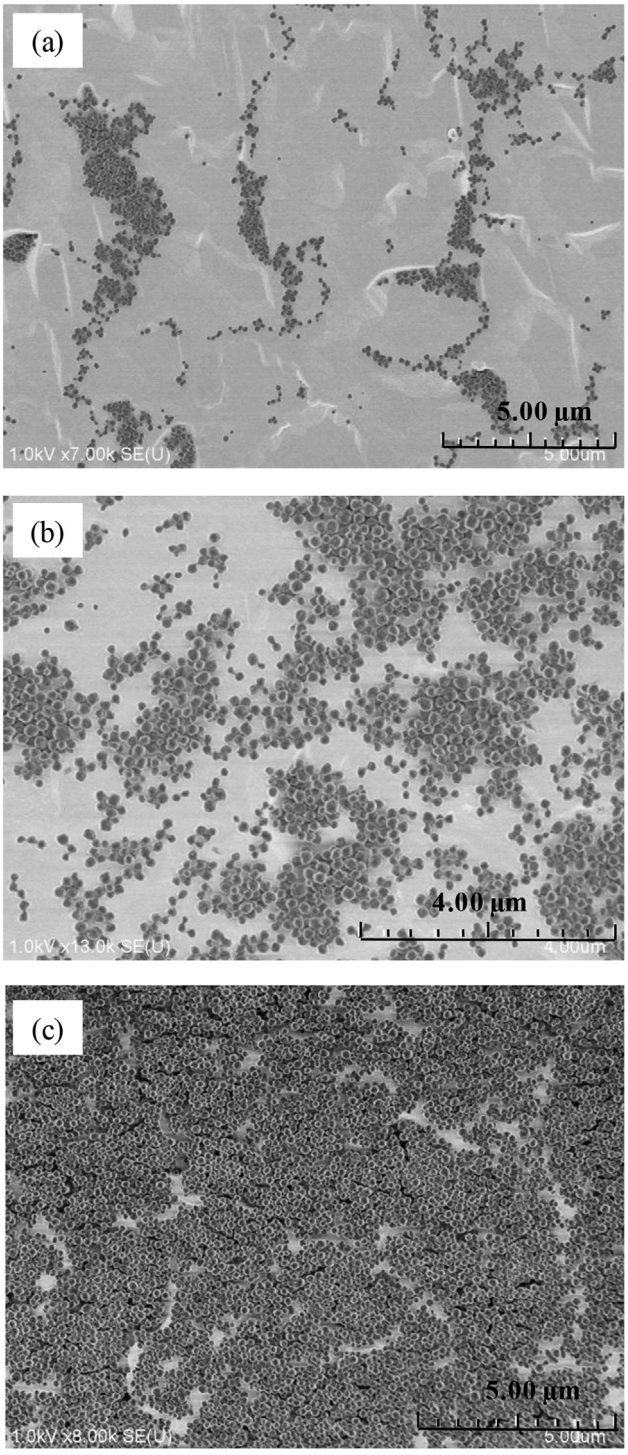

Fig. 5. SEM images of a QCM electrode coated with different nanobead concentrations: (a) 5 mg/mL, (b) 10 mg/mL and (c) 20 mg/mL.

3.3. Optimization of preparation conditions

Compared with bulk polymerization, which affords monolithic MIP materials, precipitation polymerization is not a straightforward method for imprinting template molecules because excess solvent is needed in the polymerization. The excess solvent interferes with molecular interactions between the functional monomers and the template, and thus the imprinting is less efficient and the ligand binding of the imprinted microspheres will be lower than that of a conventional monolith [42]. To obtain an optimum imprinting effect, we investigated the influence of the molar ratio between the functional monomer (MAA), the crosslinker (TRIM) and the template (HA as an example) on the sensitivity of the MIP nanobead coated QCM electrodes. The results shown in Table 1 demonstrate that the highest sensitivity ($-\Delta F/\Delta m$) was achieved with a ratio of MAA/TRIM of 1:1 (11.2 Hz/μg) and a ratio of HA/MAA with 2:1 (10.7 Hz/μg). A relatively high content of the crosslinker and the template were required compared with that of conventional bulk polymerization. For example, in our previous work on the preparation of a monolithic MIP micropowder, the optimized ratio of MAA/TRIM/HA was 3:9:1 [34]. We attributed this result to the dilution effect of excess solvent in the precipitation polymerization.

3.4. MIP effect evaluated by QCM measurements

On the basis of the optimized conditions, three MIP nanobeads (PA-, HA- and OA-) were prepared and their MIP effects on vapor absorption were compared with the NIP nanobeads by QCM measurements. Fig. 6 shows the typical response of the QCM electrodes coated with the NIP and MIP nanobeads upon exposure to individual vapors. Although the NIP electrodes showed non-specific response to each vapor, larger responses were observed for the MIP electrodes, which confirmed the imprinting effect of the template molecules. The imprinting efficiency ratio of three MIP nanobeads was calculated to be 1.80 for PA-MIP, 1.66 for HA-MIP, and 1.28 for OA-MIP, respectively. Here, the efficiency ratio is defined as the ratio between the sensitivity for the target molecules obtained with the imprinted nanobeads and that of the non-imprinted counterpart. The MIP effect tended to decrease as the size of the template molecules increased. We attribute this result to the increased chain length and decreased polarity, which weakened the hydrogen bonding interactions between the template molecules and the polymer matrix. The three MIP nanobeads showed differences in their sensitivity as well as the response/recovery dynamics. Rapid response and recovery were observed for the PA sensing while these processes were relatively slow for OA sensing. This result might be related to the different characteristics of the targeted vapor molecules, such as their molecular weight and volatility. Notably, the concentrations of the three vapors tested in this study were approximately 7.64 ppm for PA, 5.38 ppm for HA and 4.11 ppm for OA. The MIP sensor array reported in our previous work showed no response to the three vapors at such low concentration levels [41]. The concentration was estimated as from several tens to hundreds of ppm according to the generation method (volatilized from a kimwipe paper soaked with liquid samples). Moreover, the concentrations of carboxylic acid (typically acetic acid) reported by other literature are 285 ppm in Ref. [30] and 160 ppm in Refs. [31–33]. These above results verify the high sensitivity of MIP nanobeads on the carboxylic acid vapors.

3.5. MIP effect evaluated by SPEM-GC/MS measurement

Volatile molecules generally have a low molecular weight and molecular volume. When these molecules are used as a template to prepare MIP materials, the size of the imprinted cavities commonly lies at the Ångström or nanometer level. Therefore, conventional instrumental analytical methods are cannot provide meaningful structure information to support the MIP effect. For example, we investigated the surface morphology of nanobeads with an advanced field emission scanning electron microscope at a super high resolution (300,000 × magnification). Furthermore, we performed surface area analysis and pore size measurements with a high-performance gas sorption analyzer. In both cases, we could

Table 1
Influence of molar ratio between the monomer (MAA), crosslinker (TRIM) and template on the sensitivity of the MIP-nanobead-coated QCM electrode. HA was used as an example template to prepare the HA-MIP nanobeads. The concentration of HA vapors was 5.38 ppm.

MAA/TRIM (mmol/mmol)	$\Delta F/\Delta m$ (Hz/μg)	HA/MAA (mmol/mmol)	$\Delta F/\Delta m$ (Hz/μg)
1:2	6.5	2:1	6.0
1:1	11.2	1:1	7.5
2:1	6.8	2:1	10.7
3:1	2.0	3:1	8.2

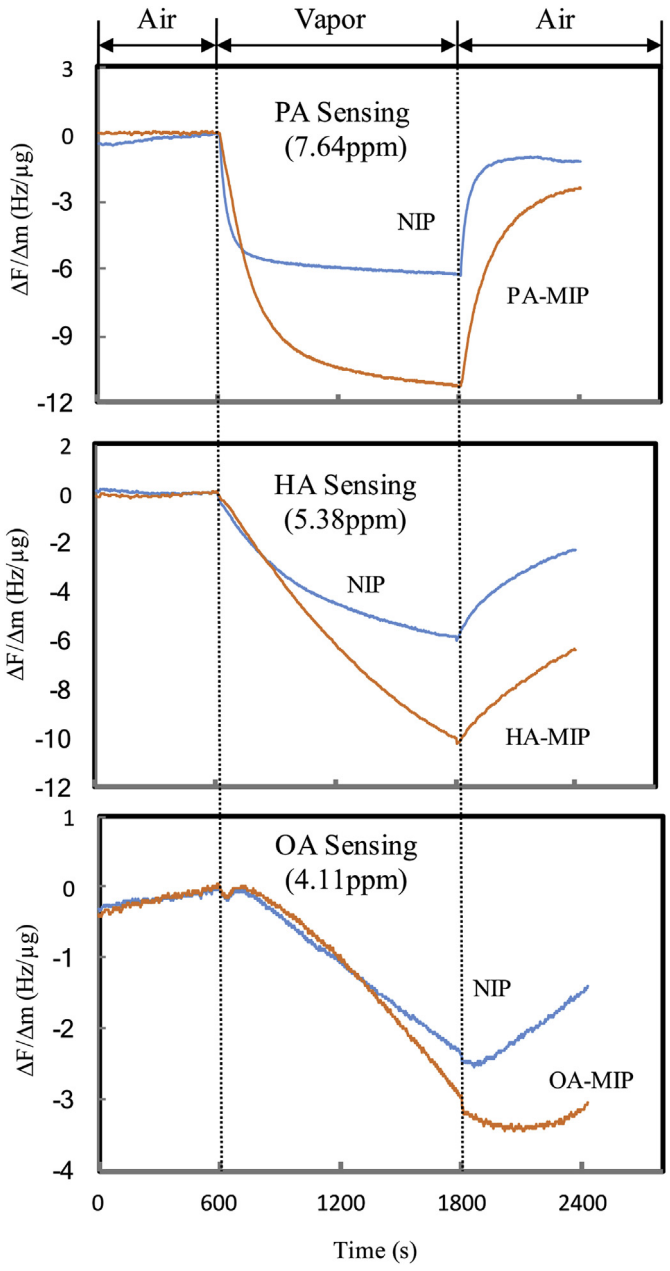

Fig. 6. Response characteristics of QCM electrodes coated with MIP and NIP nanobeads upon exposure to corresponding vapors.

not observe any obvious differences in the surface structures or pore sizes between the MIP and NIP nanobeads or among the different MIP nanobeads. The characterization of vapor absorption by FT-IR measurements also failed owing to the low concentration and high volatility of the carboxylic acid molecules. To verify the imprinting effect of the MIP nanobeads on the carboxylic acid vapors, we evaluated the absorption characteristics with the use of SPME-GC/MS measurements. After vapor absorption, the nanobead samples were transferred into a vial. The absorbed vapor was desorbed again by a specific heating program of the autosampler. The desorbed vapor in the headspace of the vial was then absorbed by the SPME probe and injected into the gas chromatograph. Fig. 7 shows the result of the MIP- and NIP- nanobeads measurements

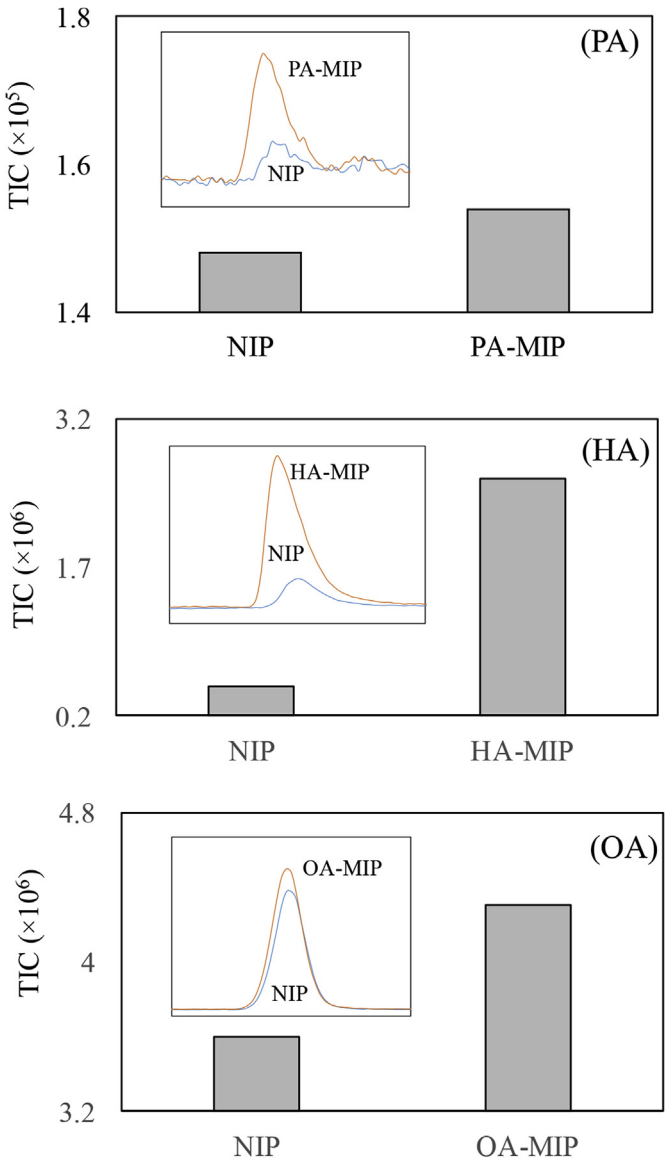

Fig. 7. SPME-GC/MS measurement result of MIP- and NIP nanobeads upon exposure to corresponding vapors. Insets shows the real gas chromatogram. Peak area of total ion current (TIC) is used in the comparison.

after the vapor absorption. The peaks corresponding to specific vapors at different retention times were identified by retrieving the mass spectra. The total ion current (TIC) values of the MIP nanobeads were then compared with that of the NIP nanobeads. All the MIP nanobeads showed higher TIC values than that of the NIP nanobeads, which indicates the effectiveness of the GC/MS measurements for evaluating the MIP effect.

3.6. Vapor discrimination by MIP-nanobead sensor array

On the basis of the NIP and three MIP nanobeads, we fabricated a four channel QCM sensor array and investigated its response characteristics to the three carboxylic acid vapors. For each vapor, three concentrations were measured and at each concentration, the measurement was repeated three times. Then, a dataset including 27 samples was collected. Fig. 8 presents the normalized sensitivity of the sensor array for all samples (mean value of three measurement with standard derivation). For each vapor, the individual MIP channel showed an enhanced response as the concentration was increased. At a given concentration, all the MIP channels showed higher sensitivity than the NIP channels. Furthermore, the response pattern of the four channel-sensor array to the three vapors were obviously different, which suggested the possibility of pattern recognition of the three vapors. To evaluate the selectivity of the sensor array, a dataset of the 27 samples was analyzed first by principle component analysis (PCA). PCA is an unsupervised method in which the samples are clustered based on similarities and differences in their PC scores. The PC score plot is shown in Fig. 9. The proportion of variance of the first three principle components were 79.1% (PC1), 16.5% (PC2), and 2.9% (PC3). The cumulative proportion of these three PCs was 98.5%, which contained the main information of the original dataset matrix. Although the vapor samples were roughly separated, partial overlapping was observed both in the PC1-PC2 space and the PC2-PC3 space, which may indicate insufficient performance of PCA. In view of this, the dataset was also analyzed by linear discrimination analysis (LDA). Unlike unsupervised PCA, LDA is a supervised classifier in which the samples are grouped by minimizing the intragroup distance and maximizing the intergroup distances simultaneously. Two discrimination functions (LDA1 and LDA2) were obtained by a linear combination of the variables of the sensor array. Fig. 10 shows the LDA score plot of the QCM sensor array's response to the three carboxylic acid vapors. All samples were plotted in the LDA space into three clusters without any overlap. Clearly, the LDA method showed better classification performance than that of the PCA method. A method based on leave-one-out-cross-validation (LOOCV) was applied to validate the LDA model. A 96% classification rate was achieved for the measured 27 samples, which demonstrates that the MIP nanobeads are effective in the detection and discrimination of carboxylic acid vapors.

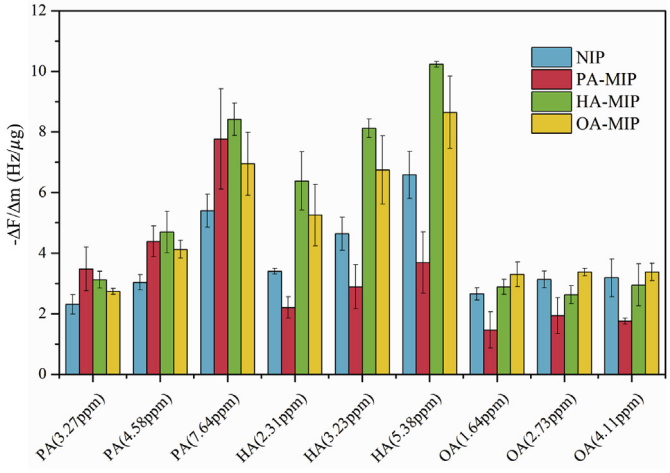

Fig. 8. Vapor response characteristics of a QCM sensor array containing four channels coated with the NIP, PA-MIP, HA-MIP and OA-MIP nanobeads, respectively. The graph shows the mean value of three measurements with error bar (standard deviation).

3.7. Comparison of different MIP material characteristics

Generally, the MIP effect observed for MIPs templated with small molecules is poorer than that of MIP materials based on large molecules as the templates [42,43]. The maximum response ratio of the MIP to NIP observed in this study was not more than two for the MIP nanobeads. Vapor (or odorant) molecules generally have features such as low molecular weight (<300 Da), small molecular size, and high volatility. In addition, for polymer-based MIP materials nonspecific absorption in the vapor phase is generally more obvious that in the liquid phase. Therefore, we suggest that it is almost impossible to prepare MIPs with a highly specific affinity for vapor, such as the recognition occurring in enzymes, antibodies, and macromolecule-templated MIPs. The human olfactory system has developed roughly 400 types of odor receptors to handle the numerous types of odorant molecules that are commonly encountered. The recognition of olfactory receptors on odorant molecules is based on global selectivity. The concept of global selectivity has been widely used in the fabrication of electronic noses. Although the imprinting efficiency ratio of the individual MIP nanobeads was not high, the result of this study proves that the global selectivity contributes to the recognition ability of the MIP nanobead sensor array. Compared with our previous work based on MIP films [41,49,50], this study represents a considerable improvement in the sensitivity. We attributed these results to the high specific surface area of the nano-sized MIP beads. Furthermore, we have recently reported molecularly imprinted sol-gels (MISGs) and their application to vapor and odorant sensing [51,52]. We proposed that for MIP materials both the matrix effects and the MIP effect have an important contribution to the recognition ability of sensor arrays for different vapors. The molecular imprinting provides further enhance of the discrimination ability of sensor array of compared with conventional sensing materials such as chromatographic adsorbents [39]. Different MIP materials (polymer and sol-gel) could also complement each other in the same way that SPME techniques are used, with polymer/molecular sieve composite membranes, to adjust the adsorption performance of the probe. Therefore, we believe that the vapor recognition ability could be further improved if a hybridized MIP sensor array can be fabricated. We are currently investigating these possibilities. We hope that the detection and characterization of human body odor consisting of a complex mixture of components (including carboxylic acids, aldehydes, ketones) can be realized through the use of various kinds of MIP materials, including polymer-MIPs, nanobead-MIP and sol-gel-MIPs among others.

4. Conclusion

To develop sensing materials for detecting various carboxylic acids contained in human body odor, molecularly imprinted polymer beads were prepared by precipitation polymerization in the presence of template molecules. The size of the prepared polymer beads was investigated by SEM at the nanometer level (150–200 nm). The molecular imprinting effect was confirmed both by QCM and GC/MS measurements through a comparison of the absorbance performance between the NIP and MIP nanobeads.

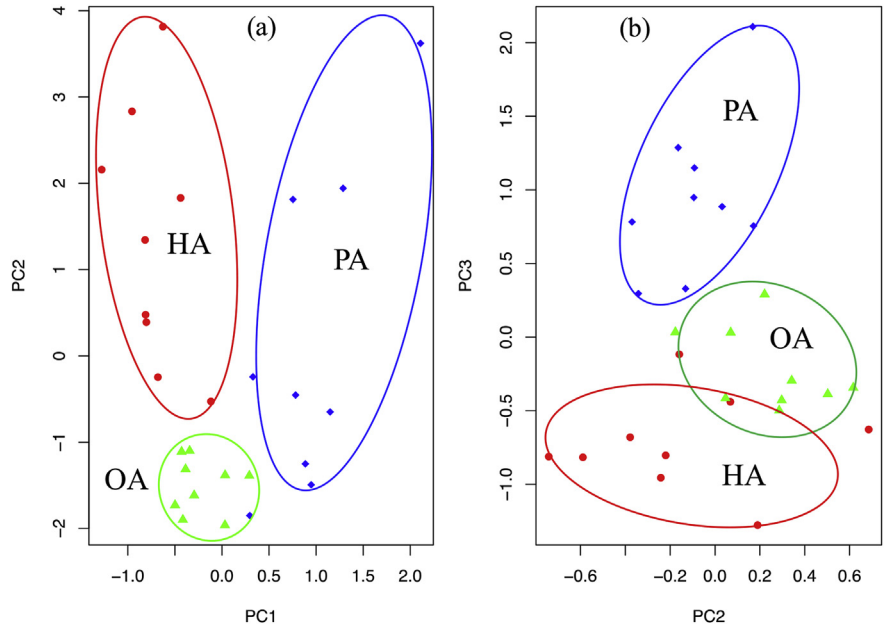

Fig. 9. PCA plots of the QCM sensor array's responses to carboxylic acid vapors in the PC1-PC2 space (a) and the PC2-PC3 space (b).

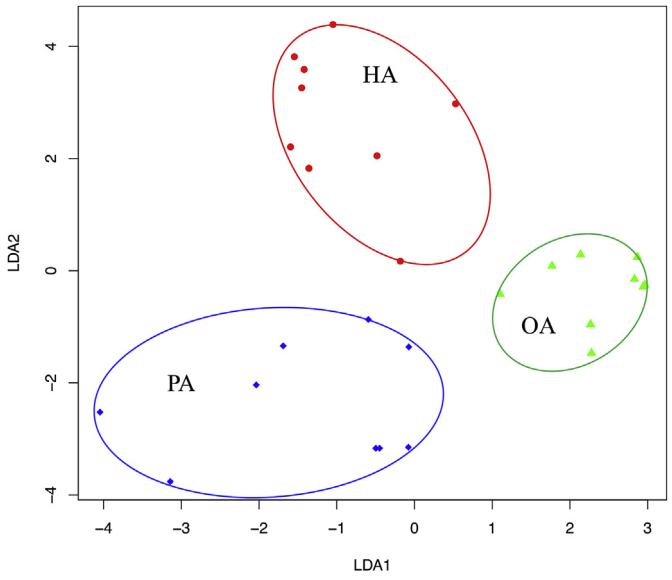

Fig. 10. LDA score plot of the QCM sensor array's responses to carboxylic acid vapors.

A QCM sensor array including one NIP channel and three MIP channels was fabricated and used to detect three typical types of carboxylic acid vapor in human body odor with concentrations at the ppm level. Both nonsupervised (PCA) and supervised (LDA) methods were applied to analyze the data from the sensor array. LDA showed a better discrimination ability than that of PCA. A 96%-classification rate was achieved through leave-one-out cross-validation technique of the LDA model. The improved performance in both sensitivity and selectivity was attributed to the imprinting and size effect of the imprinted nanobeads. The developed MIP nanobeads could be used as artificial receptors in vapor and odorant sensing.

Acknowledgements

This work was partly supported by JSPS KAKENHI Grant Number 25420409.

References

[1] D.J. Penn, E. Oberzaucher, K. Grammer, G. Fischer, H.A. Soini, D. Wiesler, et al., Individual and gender fingerprints in human body odour, J. R. Soc. Interface 4 (2007) 331–340.
[2] M. Shirasu, K. Touhara, The scent of disease: volatile carboxylic compounds of the human body related to disease and disorder, J. Biochem. 150 (2011) 257–266.
[3] E.A. Boyse, G.K. Beauchamp, K. Yamazaki, The genetics of body scent, Trends Genet. 3 (1987) 97–102.
[4] A.M. Curran, S.I. Rabin, P.A. Prada, K.G. Furton, Comparison of the volatile carboxylic compounds present in human odor using SPME-GC/MS, J. Chem. Ecol. 31 (2005) 1607–1619.
[5] J. Havlicek, P. Lenochova, The effect of meat consumption on body odor attractiveness, Chem. Senses 31 (2006) 747–752.
[6] S. Haze, Y. Gozu, S. Nakamura, Y. Kohno, K. Sawano, H. Ohta, et al., 2-Nonenal newly found in human body odor tends to increase with aging, J. Invest. Dermatol. 116 (2001) 520–524.
[7] S. Mitro, A.R. Gordon, M.J. Olsson, J.N. Lundström, The smell of age: perception and discrimination of body odors of different ages, PLoS One 7 (2012), e38110.
[8] C.S.J. Probert, T. Khalid, I. Ahmed, E. Johnson, S. Smith, N.M. Ratcliffe, Volatile carboxylic compounds as diagnostic biomarkers in gastrointestinal and liver diseases, J. Gastrointest. Liver Dis. 18 (2009) 337–343.
[9] R.M.S. Thorn, J. Greenman, Microbial volatile compounds in health and disease conditions, J. Breath Res. 6 (2012), 024001.
[10] M. Troccaz, G. Borchard, C. Vuilleumier, S. Raviot-Derrien, Y. Niclass, S. Beccucci, et al., Gender-specific differences between the concentrations of nonvolatile (R)/(S)-3-methyl-3-sulfanylhexan-1-Ol and (R)/(S)-3-hydroxy-3-methyl-hexanoic acid odor precursors in axillary secretions, Chem. Senses 34 (2009) 203–210.
[11] S. Yamazaki, K. Hoshino, M. Kusuhara, Odor associated with aging, Anti Aging Med. 7 (2010) 60–65.
[12] M. Gallagher, J. Wysocki, J.J. Leyden, A.I. Spielman, X. Sun, G. Preti, Analyses of volatile carboxylic compounds from human skin, Br. J. Dermatol. 159 (2008) 780–791.
[13] N.L.M. Kanlayavattanakul, Body malodours and their topical treatment agents, Int. J. Cosmet. Sci. 33 (2011) 3.
[14] P. Mochalski, K. Unterkofler, G. Teschl, A. Amann, Potential of volatile carboxylic compounds as markers of entrapped humans for use in urban search-and-rescue operations, Trac. Trends Anal. Chem. 68 (2015) 88–106.
[15] U.R. Bernier, M.M. Booth, R.A. Yost, Analysis of human skin emanations by gas

chromatography/mass spectrometry. 1. Thermal desorption of attractants for the yellow fever mosquito (Aedes a egypti) from handled glass beads, Anal. Chem. 71 (1999) 1–7.
[16] U.R. Bernier, D.L. Kline, D.R. Barnard, C.E. Schreck, R.A. Yost, Analysis of human skin emanations by gas chromatography/mass spectrometry. 2. Identification of volatile compounds that are candidate attractants for the yellow fever mosquito (Aedes aegypti), Anal. Chem. 72 (2000) 747–756.
[17] N. Goetz, G. Kaba, D. Good, Detection and identification of volatile compounds evolved from human hair and scalp using headspace, J. Soc. Cosmet. Chem. 39 (1988) 1–13.
[18] F. Kanda, E. Yagi, M. Fukuda, K. Nakajima, T. Ohta, O. Nakata, Elucidation of chemical compounds responsible for foot malodour, Br. J. Dermatol. 122 (1990) 771–776.
[19] M. Kubota, R. Komaki, Y. Ito, M. Arai, H. Niwase, Investigation of the odor evolved from human hair, J. Soc. Cosmet Chem. Jpn. 28 (1994) 295–298.
[20] S. Iida, N. Ichinose, T. Gomi, K. Someya, K. Hirano, M. Ogura, et al., Mechanism and regulation of body malodor generation (1), J. Soc. Cosmet Chem. Jpn. 37 (2003) 195–201.
[21] M. Miyazaki, K. Fujihira, M. Sadaie, N. Nishikawa, R. Kon, K. Sugiyama, Mechanism and regulation of body malodor generation (2), J. Soc. Cosmet Chem. Jpn. 37 (2003) 202–209.
[22] S. Chen, V. Mahadevan, L. Zieve, Volatile fatty acids in the breath of patients with cirrhosis of the liver, J. Lab. Clin. Med. 75 (1970) 622–627.
[23] G. Preti, L. Clark, B.J. Cowart, R.S. Feldman, L.D. Lowry, E. Weber, et al., Non-oral etiologies of oral malodor and altered chemosensation, J. Periodontol. 63 (1992) 790–796.
[24] W. Miekisch, J.K. Schubert, G.F. Noeldge-Schomburg, Diagnostic potential of breath analysis–focus on volatile carboxylic compounds, Clin. Chim. Acta 347 (2004) 25–39.
[25] G.S. Rao, Diagnostic potential of breath analysis in oral disease and hygiene, Clin. Chem. 29 (1983) 1692.
[26] A. Manolis, The diagnostic potential of breath analysis, Clin. Chem. 29 (1983) 5–15.
[27] A.H. Kolk, J.J. van Berkel, M.M. Claassens, E. Walters, S. Kuijper, J.W. Dallinga, et al., Breath analysis as a potential diagnostic tool for tuberculosis, Int. J. Tubercul. Lung Dis. 16 (2012) 777–782.
[28] A.G. Singer, G.K. Beauchamp, K. Yamazaki, Volatile signals of the major histocompatibility complex in male mouse urine, Proc. Natl. Acad. Sci. U. S. A. 94 (1997) 2210–2214.
[29] S.K. Pandey, K.-H. Kim, Human body-odor components and their determination, TrAC Trends Anal. Chem. 30 (2011) 784–796.
[30] S. Ko, J. Jang, Controlled amine functionalization on conducting polypyrrole nanotubes as effective transducers for volatile acetic acid, Biomacromolecules 8 (2007) 182–187.
[31] T. Gao, E.S. Tillman, N.S. Lewis, Detection and classification of volatile carboxylic amines and carboxylic acids using arrays of carbon black-dendrimer composite vapor detectors, Chem. Mater. 17 (2005) 2904–2911.
[32] E.S. Tillman, N.S. Lewis, Mechanism of enhanced sensitivity of linear poly (ethylenimine)-carbon black composite detectors to carboxylic acid vapors, Sens. Actuat. B 96 (2003) 329–342.
[33] E.S. Tillman, M.E. Koscho, R.H. Grubbs, N.S. Lewis, Enhanced sensitivity to and classification of volatile carboxylic acids using arrays of linear poly(ethylenimine)-carbon black composite vapor detectors, Anal. Chem. 75 (2003) 1748–1753.
[34] S.Y. Kazuya Iwata, Hiro-Taka Yoshioka, Chuanjun Liu, Kenshi Hayashi, Preparation of fluorescent molecularly imprinted polymer micropowder for odorant visualization, Sens. Mater. 28 (2016) 6.
[35] C.J. Liu, Y. Furusawa, K. Hayashi, Development of a fluorescent imaging sensor for the detection of human body sweat odor, Sens. Actuat. B 183 (2013) 117–123.
[36] N.C. Speller, N. Siraj, S. Vaughan, L.N. Speller, I.M. Warner, Assessment of QCM array schems for mixture identification: citrus scented odors, RSC Adv. 6 (2016) 95378–95386.
[37] A. Tuantranont, A. Wisitsora-at, P. Sritongkham, K. Jaruwongrungsee, Anal. Chim. 687 (2011) 114–128.
[38] X. Jin, Y. Huang, A. Mason, Multichannel quartz crystal microbalance gas sensor array, Anal. Chem. 81 (2009) 595–603.
[39] M.E. Escuderos, S. Sánchez, A. Jiménez, Application of a quartz crystal microbalance (QCM) system coated with chromatographic adsorbents for the detection of olive oil volatile compounds, J. Sens. Tech. 1 (2011) 1–8.
[40] Y. Zhang, D. Chen, Multilayer Integrated Film Bulk Acoustic Resonators, Springer, Berlin Heidelberg, 2013.
[41] S.K. Jha, C.J. Liu, K. Hayashi, Molecular imprinted polyacrylic acids based QCM sensor array for recognition of carboxylic acids in body odor, Sens. Actuat. B 204 (2014) 74–87.
[42] L. Ye, R. Weiss, K. Mosbach, Synthesis and characterization of molecularly imprinted microspheres, Macromolecules 33 (2000) 8239–8245.
[43] P.A.G.C.a.K.M. Lei Ye, Molecularly imprinted monodisperse microspheres for competitive radioassay, Anal. Commun. 36 (1999) 3.
[44] S. Slomkowski, J.V. Alemán, R.G. Gilbert, M. Hess, K. Horie, R.G. Jones, et al., Terminology of polymers and polymerization processes in dispersed systems (IUPAC Recommendations 2011), Pure Appl. Chem. 83 (2011) 2229–2259.
[45] A. Poma, A.P.F. Turner, S.A. Piletsky, Advances in the manufacture of MIP nanoparticles, Trend Biotech. 28 (2010) 629–637.
[46] S.Z. Bajwa, G. Mustafa, R. Samardzic, T. Wangchareansak, P.A. Lieberzeit, Nanostructured materials with biomimetic recognition abilities for chemical sensing, Nanoscale Res. Lett. 7 (2012).
[47] G. Vasapollo, R.D. Sole, L. Mergola, M.R. Lazzoi, A. Scardino, S. Scorrano, et al., Molecularly imprinted polymers: present and future prospective, Int. J. Mol. Sci. 12 (2011) 5908–5945.
[48] S. Li, Y. Ge, S.A. Piletsky, J. Lunec, Molecularly Imprinted Sensors: Overview and Applications, Elsevier, 2012.
[49] S.K. Jha, K. Hayashi, A quick responding quartz crystal microbalance sensor array based on molecular imprinted polyacrylic acids coating for selective identification of aldehydes in body odor, Talanta 134 (2015) 105–119.
[50] S.K. Jha, K. Hayashi, Polyacrylic acid polymer and aldehydes template molecule based MIPs coated QCM sensors for detection of pattern aldehydes in body odor, Sens. Actuat. B 206 (2015) 471–487.
[51] C. Liu, B. Wyszynski, R. Yatabe, K. Hayashi, K. Toko, Molecularly imprinted sol-gel based QCM sensor array for detection and recognition of volatile aldehydes, Sensors 17 (2017) 382–397.
[52] L. Shang, C. Liu, M. Watanabe, B. Chen, K. Hayashi, LSPR sensor array based on molecularly imprinted sol-gels for pattern recognition of volatile carboxylic acids, Sens. Actuat. B 249 (2017) 14–21.